WCAP-16606-NP
Revision 0
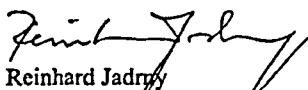
August 2006

Supplement 2 to BISON Topical Report RPA 90-90-P-A

⊛ Westinghouse

WCAP-16606-NP
Revision 0

Supplement 2 to BISON Topical Report RPA 90-90-P-A

Hakan Svensson
Safety Analysis & Structural Verification

August 2006

Reviewer: Reinhard Jadrny
Safety Analysis & Structural Verification

Approved: Lars Paulsson, Manager   *for.*
Safety Analysis & Structural Verification

Electronically Approved Records Are Authenticated in the Electronic Document Management System

ABSTRACT

The main purpose of this second supplement to the BISON topical report, RPA 90-90-P-A, "BISON – One Dimensional Dynamic Analysis Code for Boiling Water reactors," Reference 1, is to document how BISON, in combination with an approved containment code, can be used to calculate a conservative containment response during an anticipated transient without scram (ATWS).

To enable such calculations, the following three perspectives need to be described, none of which were covered in the original topical report for BISON, Reference 1, or the first supplement, CENPD-292-P-A, "BISON – One Dimensional Dynamic Analysis Code for Boiling Water Reactors: Supplement 1 to Code Description and Qualification," Reference 2. These new perspectives covered by the second amendment are:

- To increase the maximum approved upper pressure and steam quality limit with respect to the void correlation used.

- To add reactivity impact from Boron during transients.

- To provide an example of an ATWS calculation using the BISON code.

TABLE OF CONTENTS

WCAP-16606-NP
      August 2006
      Revision 0

LIST OF TABLES

LIST OF FIGURES

ACRONYM

1D	Modeling core with single channel and one dimensional kinetics
3D	Modeling core with parallel channels and three dimensional kinetics
ARI	Alternate Rod Insertion
ATWS	Anticipated Transients Without Scram
Bconc	Boron weight concentration in Boron solution
BISON	Westinghouse transient analysis 1D code, see Reference 1
Bmass	Total available Boron Solution mass that can be inserted
BOC	Beginning of Cycle
Bppm	Boron concentration in the reactor water
Bppm0	Initial (steady state) Boron concentration in the reactor water
CPR	Critical Power Ratio
CRD	Control Rod Drive System
D1	Fast diffusion constant
D2	Thermal diffusion constant
D4.1.2	Westinghouse SVEA-96 Optima2 CPR correlation
DC	Downcomer
EB	Boron efficiency factor
EBc	Boron conservativeness factor
EB3d	Boron 3D core correction factor
EOFP	End of Full Power·
EOP	Emergency Operating Procedures
EFPH	End of Full Power Hours
FSAR	Final Safety Analysis Report
GOTHIC	Containment analysis code
HPCI	High Pressure Coolant Injection System
HSBW	Hot Shutdown Boron Weight
k_{eff} (0 ppm)	k_{eff} with no Boron concentration
k_{eff} (x ppm)	k_{eff} with a Boron concentration of x ppm
LTR	Licensing Topical Report
MB	Total inserted Boron solution
MBe	Total effectively inserted Boron solution
mBs	Boron solution flow rate
MOC	Middle of Cycle
Mrpv	Total water mass in the rector pressure vessel including the drive loops
MSIV	Main Steam Isolation Valve
ntot	Total number of thermal hydraulic volumes in BISON
OLMCPR	Operating Limit Minimum Critical Power Ratio
pcm	Percent million
POLCA7	Westinghouse in core fuel management 3D code
ppm	Parts per million
PRFO	Pressure Regulator Failure, Open to maximum demand
RCIC	Reactor Core Isolation Cooling system
RPT	Recirculation Pump Trip
RPV	Reactor Pressure Vessel

ACRONYM (cont.)

SER	Safety Evaluation Report
SLCS	Standby liquid control system
SLMCPR	Safety Limit Minimum Critical Power Ratio
TBV	Turbine Bypass Valve
TCV	Turbine Control Valve
$V(i)$	Volume of thermal hydraulic volume i
$\alpha(i)$	Void fraction in thermal hydraulic volume i
Δk_{eff}	Differential impact on k_{eff} from Boron
$\rho_f(i)$	Density of water in thermal hydraulic volume i
Σ	Nuclear cross-section or diffusion constant
$\Sigma base$	Nuclear cross-section or diffusion constant derived as described in References 1 and 3, all described methods can be used
ΣB	Nuclear cross-section or diffusion constant for the second data set with Boron
ΣnB	Nuclear cross-section or diffusion constant for the second data set without Boron
$\Sigma a1$	Fast absorption cross-section
$\eta\Sigma f1$	Fast fission cross-section times yield
$\Sigma r1$	Removal cross-section
$\Sigma a2$	Thermal absorption cross-section
$\eta\Sigma f2$	Thermal fission cross-section times yield

1   INTRODUCTION

The Westinghouse transient analysis methods are described in the Licensing Topical Reports (LTRs) RPA 90-90-P-A, "BISON – One Dimensional Dynamic Analysis Code for Boiling Water Reactors," Reference 1, and CENPD-292-P-A, "BISON – One Dimensional Dynamic Analysis Code for Boiling Water Reactors: Supplement 1 to Code Description and Qualification," Reference 2.

RPA 90-90-P-A describes the BISON transient code and the code qualification for BWR transient analyses and was approved for use in license applications by the U.S. NRC in 1989. CENPD-292-P-A was submitted to introduce changes and upgrades to the methods in order to address some of the SER conditions on the original LTR. The second LTR was approved in 1995.

The transient analysis design bases and overall reload methodology are summarized in the Reference Safety Analysis Report for BWR Reload Fuel, Reference 3. The methodology is currently used by Westinghouse for introducing new fuel designs into nuclear power plants in the US.

The main purpose of the second supplement to the BISON topical report, Reference 1, is to extend the applicability of the code to the analysis of ATWS sequences beyond the peak pressure calculations performed today and to determine the mass and energy release to the containment during the Boron injection phase of the accidents.

This report is structured to complement and augment the original LTR and its supplement described above with the following specific features:

- To extend the maximum approved upper pressure and steam quality limit for the AA78 slip/void correlation.

- To model the reactivity impact from Boron injection during an ATWS transient.

- To describe an example of ATWS calculations during the Boron injection phase with the BISON code.

The AA78 slip/void correlation was qualified up to a pressure of 10 MPa (1450 psia) in Reference 1 by comparing the results obtained with the AA78 slip/void correlation to the results obtained using the EPRI slip/void correlation described in Reference 7. NRC SER Condition 4 in the topical report RPA 90-90-P-A requires justification if the AA78 slip/void correlation is used above 1450 psia. The approved range of applicability covers most of BWR applications in the US, including the ASME over pressurization analyses. However, the peak pressure acceptance criterion for the ATWS analysis at BWR/3 plants [   ]^{a,c} is as high as [   ]^{a,c} and therefore it is necessary to extend the range of application of the slip/void correlation to cover pressures above 1450 psia. The justification of the AA78 correlation extension is given in Chapter 3.

The Boron concentration model is described in Chapter 4, its validation in Chapter 5 and the example how to use the model in Chapter 6.

2   THE BASIC MODEL

The physical and thermal-hydraulic models of the BISON code are described in Reference 1, Chapters 2 and 3. Amendments to the model are described in Reference 2.

Boron solution is not accounted for in the thermodynamic model since the Boron solution volume flow is not added to the volume of the water in the Reactor Pressure Vessel Model. Hence all descriptions of the physical model and the thermal-hydraulics as presented in References 1 and 2 are unaffected by the introduction of the present Boron model.

The neutron kinetics model and the different methods available to generate cross-sections for the kinetics model are described in Reference 1, Chapter 4 and are modified with this supplement. In the kinetics model an additive Boron reactivity model will be used. Additional details are provided in Chapter 4.2.

3 JUSTIFICATION FOR SLIP AND VOID CORRELATION IF PRESSURE EXCEEDS 1450 PSIA

The AA78 slip correlation is described in the BISON Topical Report, Reference 1. This correlation is basically a bubble flow correlation modified to cover annular flow as well as for BWR fuel bundles. The mass flux enters explicitly and the pressure only via pressure dependent thermodynamic quantities.

The correlation is a best fit to void measurements performed with full-scale (36 and 64 rods) test sections in the Westinghouse FRIGG test loop. The original recommended range of applicability was:

Pressure: 3.0 to 9.0 MPa (435 to 1305 psia)
Mass flux: 500 to 2900 kg/m^{2}s (0.30 to 2.1 Mlb/h-ft^2)
Steam quality: 0 to 1.0

Covered ranges in these early FRIGG void measurements were:

Table 3-1	Covered Ranges in the AA78 Data Base			
Test Section	Pressure (MPa)	Mass Flux (kg/m^{2}s)	Steam Quality (%, max)	Void Fraction (%, max)
0F-36	3.0-9.0	550-2900	40	90
0F-64A	4.8, 6.8	500-2500	40	90
0F-64B	6.8	500-2000	55	95

Additional void measurements were later performed for SVEA-96 geometries (sub-bundle test sections) with lower mass flux values and extended the lower limit to 400 kg/m^{2}s. The void predicted by the AA78 correlation was compared to these new measurements and extrapolation below the data range for mass flux is considered acceptable at least down to 400 kg/m^{2}s.

This new data covered the following ranges:

Table 3-2	Additional Void Measures Utilized for Verification & Validation of the AA78 Void Correlation				a,b,c

The error distribution and standard deviation for the AA78 void correlation as a function of the void is shown in Table 3-3 and the comparison against each measurement series in Table 3-4.

Table 3-3	Error Distribution as a Function of the AA78 Predicted Void		a,c

Table 3-4	Mean Error and Standard Deviation of the AA78 Predicted Void Compared to the Measured Void for the Different Series			a,b,c

EPRI Void Correlation

The EPRI void correlation is based on a larger data base which includes not only rod bundle measurement but also measurements from heated rectangular channels and round tubes. The description of the correlation is given in Reference 6. The statistical Analysis of the Model versus Data for the different types of measurements is provided in Tables 3, 8, and 11 of the EPRI report and summarized in the following table. In addition, Table 13 in Reference 6 gives the Model versus Data – Pressure and Flow Range Comparison and is shown in Figures 3-1 and 3-2 for information.

Table 3-5	Mean Error and RMS Error of the EPRI Predicted Void Compared to the Measured Void for the Different Type of Experimental Data		
Experimental Data	Mean Error	RMS Error σ	Sample Size
Rod Bundles	-0.0002 ± 0.0010	0.028	784
Rectangular Channels	-0.0021 ± 0.0018	0.051	776
CISE Tube Data	-0.0007 ± 0.0010	0.022	440

During the NRC review of the BISON Topical Report Reference 1, questions regarding the void models were discussed further. Some of the information provided in responses to the Request for Additional Information is relevant to the discussion of the applicability of the correlation to pressures higher than 9 MPa.

Question 5 regarding the limitations of several correlations, AA78 among them, was answered in Reference 1 pages Q5-1 to Q5-6 and included comparisons with FRIGG loop data. The following text has been extracted from the answer regarding the AA78 void correlation.

"The verified data range covers most BWR applications. However, in some extreme cases, such as design basis pressurization transients (MSIV closure without position scram) or trip of all recirculation pumps, the limits of the above data range may be exceeded. However, the dependencies in pressure and mass flux are smooth and continuous, and the correlation prediction outside the above range follows the expected trend."

To justify that extrapolation beyond the test conditions is acceptable two figures, Q5.1 and Q5.2, were provided. Figure Q5.1 plots measured void against steam quality for two pressures, 7 and 9 MPa (1015 and 1305 psia), at the same inlet subcooling. Also shown are the BISON calculated curves for various pressures. These calculated curves show that there is a smooth trend in void as a function of pressure. Figure Q5.2 shows measured versus calculated void at different pressures, and demonstrate that there is no significant trend in the error as a function of pressure.

Question Q24 requested further justification of the use of the void and boiling correlations in BISON at pressures higher than 9 MPa.

Comparison with other correlations with somewhat larger range of applicability has verified that the correlation behavior is also correct outside the above ranges. Further discussion and justification is provided by the answer to NRC Question 24 in Reference 1, pages Q24-1 to Q24-6. Comparative graphs of pressure trends up to 10.0 MPa and steam qualities up to [   ]^{a,c} were presented. The graphs compare void change trends predicted with AA78 combined with the Solberg boiling/condensation model and with the Lellouche-Zolotar EPRI slip correlations described above.

The EPRI correlation has been verified for a wide range of pressures. It was developed to fit not only the rod data which forms the basis of the AA78 correlation, but also other data including measurement in rectangular channel experiments at 10.3 and 11.0 MPa (1493 and 1598 psia). Thus, it serves as a reference for the variation of void fraction with pressure for a range of geometries.

The following text has been extracted from the answer to Question 24:

"... Figure Q24.1 shows the total change of void fraction with increasing pressure starting at 7 MPa, at constant steam quality, as calculated using the Lellouche-Zolotar correlation, for typical BWR channel conditions. For example, at steam quality 0.2, the void fraction at 8 MPa is approximately 0.025 smaller than that at 7 MPa, and at 10 MPa, the void fraction is approximately 0.075 smaller than that at 7 MPa.

Comparison of this figure with the corresponding curves calculated with AA78 and the Solberg models using parameters derived for a single channel application (Figure Q24.2), and using parameters for application to core average conditions (Figure Q24.3), and also with curves calculated using the modified Bryce-Holmes correlation (Figure Q24.4), indicates that the change of void fraction with pressure over the range 7 to 10 MPa is the same for all methods."

The application of the AA78 void correlation to pressures up to 10 MPa was justified through the answer to Questions Q5 and Q24.

The matter was further discussed in the first supplement to Topical Report, Reference 2. This supplement to the BISON topical report was submitted, among other improvements, to change the boiling and condensation model (core void profile) from Solberg to EPRI. The EPRI boiling/condensation model is a more mechanistic, generic model and independent of the fuel type while the Solberg model is an empirically fit formulation requiring specification of three constants. The selection of these constants assured that the BISON axial coolant density matched the POLCA7 three dimensional core simulator calculated average profile.

The qualification was provided in Section 6.5.3.2 (comparison against the Peach Bottom Turbine Trip data) and in Appendix A in the answer to NRC Question A1 in Reference 2. The same qualification as the one performed in response to Question Q5 in Reference 1 was repeated for the EPRI boiling/condensation model in combination with the AA78 slip (void) correlation. The results of the prediction against the FRIGG loop data are presented in Figures A1-1 and A1-2. These figures show that the correlations give comparable results with no systematic deviations over the entire range of void fractions up to 93%.

To calculate the pressure response during an ATWS up to the acceptance criterion of [$]^{a,c}$ psia, a relative small increase in the approved maximum pressure extrapolation is required (about [
$]^{a,c}$). To avoid similar problems in the future, a new upper limit of [
$]^{a,c}$ is suggested. This range increase is supported by extended comparative graphs of the same type as the ones presented in the answer to Question 24 in Reference 1, and are shown in Figures 3-1 and 3-2.

The two differential voids versus steam quality figures for AA78 and EPRI respectively, show that both correlations have exactly the same trends. The differential void at 8.0 MPa (compared to 7.0 MPa) has its maximum at about [

$$]^{a,c}$$

The AA78 correlation is, as shown above, verified against measured data for pressures up to 9.0 MPa. In Figure 6-4 of Reference 2, the RMS error of the AA78 correlation as implemented in BISON is [$]^{a,c}$ by direct comparisons to measurement data. The mean error is [$]^{a,c}$. When extrapolating further, a comparison with the EPRI correlation is used.

The EPRI void correlation (equivalent to the Chexal-Lellouche drift flux correlation) is described in Reference 8. In this paper, void fraction results were compared to a wide range of experimental data with various geometry, inlet subcooling, power distribution, and pressure values (up to 15 MPa = 2176 psia).

Comparing the differential void changes versus [

]^{a,c} generates the following graphs:

a,c

[

]

As can be noted, [   ]^{a,c} with increasing pressure.
[

]^{a,c}

P ≤ 9.0 MPa   [   ]^{a,c}

RMS Error: [   ]^{a,c}

Mean Error   [   ]^{a,c}

As can be noted the [
                    ]^{a,c}.

The major explanation for [

]^{a,c} At increased pressure the steam/water density ratio changes with well known pressure dependence (from steam/water tables) for both correlations.

The conclusion of the comparison against experimental data provided in the answer to Questions Q5 and Q24 in Reference 1 demonstrates that there is a smooth trend in void as a function of the pressure and that there is no significant trend in the error as a function of pressure. Therefore there is not a significant increase in the uncertainties due to extrapolation of the correlation to pressures higher than those included in the data base (up to 9 MPa). This is confirmed by comparing the AA78 void to other void correlations based on experimental data for a wider range of pressures, similar to the EPRI void correlation which includes measurements up to 11 MPa. Also Table 13 in Reference 6 shows the lack of trend in the Model versus Data bias with pressure. The comparison between AA78 void correlation to other methods as

shown in Figures Q24.1 to Q24.4, and also presented in Figures 3-1 and 3-2, indicate that the change in void fraction with pressure predicted over the range 7 to 12 MPa is the [   ]^{a,c}.

At uprated power conditions with increased flow window, the core average void is expected to increase since the core average power is higher even though the sub-cooling also increases due to increased feed water flow. However, the highest void fractions occur in the hot channels. The hot channels at EPU conditions still have about the same exit void fraction, since they are limited by the thermal limits, e.g., CPR, that limit the bundle power. At EPU conditions the highest power channels have practically unchanged exit void fractions. The main difference at uprated power conditions is that more channels have higher powers.

For this reason, all correlations valid at high voids (e.g., AA78 which is based on rod bundles void measurements up to 93% void) are still within range at EPU conditions. Further justification of the applicability of the void correlation to EPU conditions and the comparison of the POLCA7 predicted void to the more recent FRIGG measurement for SVEA-96 Optima2 is provided in the answer to Question 13 in Reference 9.

a,c

Figure 3-1 Comparisons of Void Changes as a Function of Steam Quality at Different Pressures

EPRI VOID CORRELATION AND EPRI BOILING MODEL
Differential Void vs. Steam Quality
G 1000 kg/sm2 - DT Deg C - ref. Pres. 7 MPa
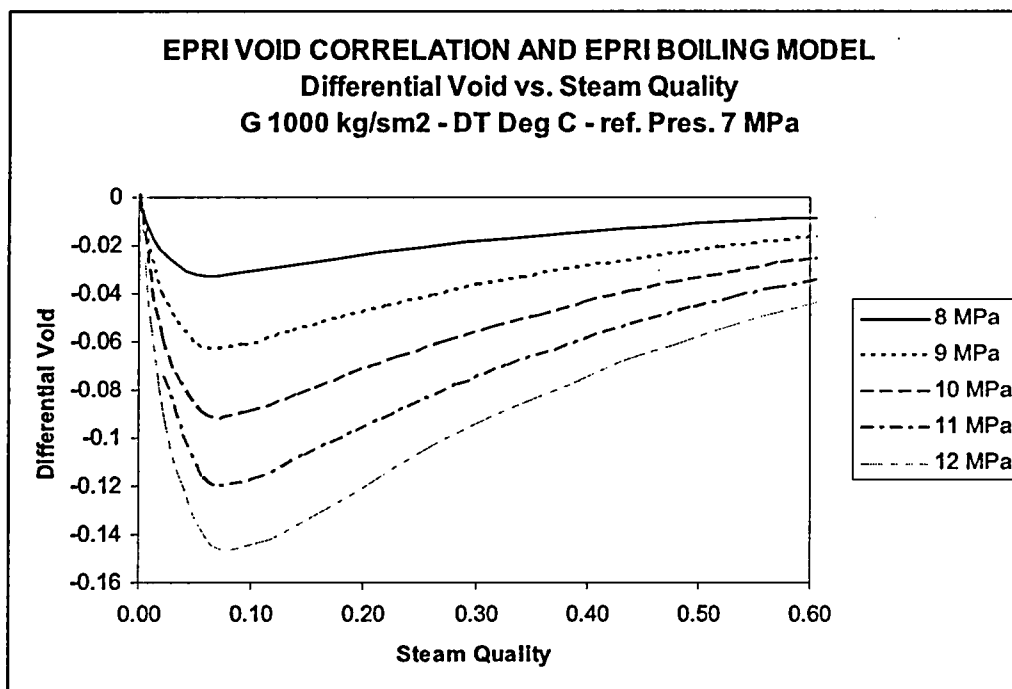
Figure 3-2 Comparisons of Void Changes as a Function of Steam Quality at Different Pressures

4   THE BORON MODEL

4.1   BORON CONCENTRATION MODEL

The Boron concentration model calculates the Boron concentration in the reactor vessel based on a Boron solution insertion flow rate, a Boron mass fraction, an available total Boron solution mass, a methodology penalty factor and a core simulator correction factor to account for actual core contents and 3D effects in the Boron reactivity worth.

To obtain the concentration of Boron in the reactor pressure vessel a conservative approach denoted "perfect mixing" is used. In this model the total water volume is used to derive the concentration based on the total water mass in the reactor vessel.

[

$]^{a,c}$ This conservative approach is explained in detail for the application example in Section 6 of this report.

[

$]^{a,c}$ the "perfect mixing" model will generate a conservative Boron concentration in the core.

4.1.1   Available Boron Mass in the System

The following parameters are given as input to the Boron injection model in BISON:

[

$]^{a,c}$

The total inserted Boron solution, MB, at any given time t is now:

$$MB = Bconc * min(Bmass, (\int_0^t mBs * dt))$$ (4.1)

To assure conservative calculations an additional factor, EB, always less than one, is also applied and an effective total amount of inserted Boron, MBe, is calculated as:

$$MBe = EB * MB$$ (4.2)

EB accounts for two different effects:

[

]^{a,c}

At each time t during the transient the total water mass Mrpv is calculated as:

$$Mrpv = \sum_{i=1}^{ntot} v(i) * (1 - \alpha(i)) * \rho_f(i)$$ (4.4)

where

ntot	total number of thermal hydraulic volumes in BISON	(-)
v(i)	volume of thermal hydraulic volume i	(m³)
α(i)	void fraction in thermal hydraulic volume i	(-)
ρ_f(i)	density of water in thermal hydraulic volume i	(kg/m³)
Mrpv	total water mass in the reactor pressure vessel including the drive loops	(kg)

4.1.2 Boron Concentration Model

The Boron concentration in ppm, Bppm, is calculated as:

$$Bppm = 1.E6 * MBe / Mrpv$$ (4.5)

This concentration is transferred to the kinetics model to calculate the reactivity impact from Boron.

To simplify comparisons with static codes (3D core simulators, e.g., POLCA7) of Boron reactivity impact, the possibility to give the initial Boron concentration (steady state) as input to the BISON code is added. This parameter, Bppm0, modifies Equation 4.5 to:

$$Bppm = Bppm0 + 1.E6 * MBe / Mrpv \tag{4.6}$$

Combining Equations (4.1) to (4.6), we now obtain:

$$Bppm = Bppm0 + \frac{1.E6 * EBc * EB3d * Bconc * \min(Bmass, (\int_0^t mBs * dt))}{\sum_{i=1}^{ntot} v(i) * (1 - \alpha(i)) * \rho_f(i)} \tag{4.7}$$

4.2 NEUTRON KINETICS MODEL

The Neutron kinetics model as described in Section 4 in Reference 1 is not changed with respect to basic equations and nuclear cross-section models.

In addition to the description in Reference 1, [

]^{a,c}. A short summary of the kinetics model described in Reference 1 is given in Section 4.2.1 below.

4.2.1 Basic Model

The neutron kinetics model used in BISON is a time-dependent two-group diffusion model with one-dimensional (axial) space dependence. The neutron kinetics properties of the reactor core are calculated from local cross-sections and delayed neutron data.

Prior to a transient calculation, a steady state is initialized by iterations between the neutron kinetics model and the thermal–hydraulics model until the power distribution and the void and temperature distributions correspond to each other.

Nuclear cross-sections are provided as polynomial functions with a set of coefficients $C_{i,j}$ as described below.

The nomenclature used for the neutron parameters is described as follows:

D_1	Fast diffusion constant	(cm)
Σ_{a1}	Fast absorption cross-section	(cm^{-1})
$\eta\Sigma_{f1}$	Fast fission cross-section times yield	(cm^{-1})
Σ_{r1}	Removal cross-section	(cm^{-1})
D_2	Thermal diffusion constant	(cm)
Σ_{a2}	Thermal absorption cross-section	(cm^{-1})
$\eta\Sigma_{f2}$	Thermal fission cross-section times yield	(cm^{-1})
Σ_{base}	Short hand notation for ANY of the above cross-sections	(different)

Independent variables:

ρ_k Average moderator density in the region/subsection k

α_k average void content (steam volume fraction) at the outlet of subsection k

T_{mk} Moderator temperature assumed equal to the coolant liquid temperature in subsection k

T_f Mean fuel temperature

T_f^0 Reference fuel temperature

T_m^0 Reference moderator temperature

ΔT_m $T_{mk} - T_m^0$

General polynomial form:

$$\sum\nolimits_{base} = C_{i1} * (1 + C_{i,5} * \Delta T_m) + C_{i,2} * (1 + C_{i,6} * \Delta T_m) * \rho_k +$$
$$C_{i3} * (1 + C_{i,7} * \Delta T_m) * \rho_k^2 +$$
$$C_{i4} * (1 + C_{i,8} * \Delta T_m) * \rho_k^3 + \tag{4.8}$$

Doppler Correction:

$$\sum\nolimits_{r1} = \sum\nolimits_{r1}(T_f^0) + C_{1,9} * (1 + C_{1,10} * \rho_k + C_{1,11} * \rho_k^2) * (\sqrt{T_f} - \sqrt{T_f^0}) \tag{4.9}$$

$$\sum\nolimits_{a1} = \sum\nolimits_{a1}(T_f^0) + C_{2,9} * (1 + C_{2,10} * \rho_k + C_{2,11} * \rho_k^2) * (\sqrt{T_f} - \sqrt{T_f^0}) \tag{4.10}$$

The Doppler correction includes the fuel temperature influence on Δk from all cross-sections, although only $\sum_{r1}$ and $\sum_{a1}$ are changed in the polynomials. These corrections are calculated by the interface program.

A complete set of polynomials is provided for fuel with no control rods present, and another set with control rods fully inserted for each fuel type.

4.2.2 Boron Cross-Sections

This chapter describes the changes in the neutron kinetics model implemented in order to account for Boron in the model.

The Boron reactivity impact in BISON is assumed to be independent of the fuel or core as long as the ppm value is calculated properly. In order to catch fuel, core and state point specific impact, [

]^{a,c} is provided.

To determine the impact of Boron reactivity, [

]^{a,c}

[

]^{a,c}

The Boron cross-section model has the following dependencies for each cross-section:

$$\Sigma = \Sigma(\rho_c, \rho_{bp}, T_c, Bu, Bppm) \qquad (4.12)$$

where

ρ_c	coolant density in the core/bundles	(kg/m^3)
ρ_{bp}	coolant density in the bypass	(kg/m^3)
T_c	coolant temperature	(K)
Bu	burnup	(MWd/kgU)
Bppm	Boron concentration	(ppm)

[

]^{a,c}

[

]^{a,c} is described along with the verification and validation presented in Chapter 5 and used in an application in Chapter 6 of this report.

5 BORON REACTIVITY MODEL VERIFICATION AND VALIDATION

5.1 PURPOSE

To verify that the Boron reactivity model is correctly implemented in BISON a comparison is made against the 3D core simulator POLCA7, Reference 10.

The verification is performed at a typical initial power and recirculation flow when the Boron injection is initiated at a number of different state points and two different cycles.

The verification is also an example of how to obtain the EB3d correction factor based on parallel channels and 3D neutronics. The correction described by Equation 4.3 is applied for different cycle exposures and for different cycles. The use of such a correction factor is further demonstrated and described in Chapter 6 of this report.

The BISON Boron cross-section model uses a SVEA-100 full length fuel as reference fuel. The correct fuel types corresponding to the actual core are hence not modeled explicitly in the cross-sections used by BISON.

The impact of different cores and fuel designs as well as different plants, is taken into account by the 3D normalization factor EB3d. For the normal reactivity based on void and fuel temperatures etc, "method B" as described in Reference 1 is used.

5.2 SELECTED CORES AND STATE POINTS

The state point for this application is selected to be a typical state point just prior to the start of Boron injection for the selected plant. This state point is:

- Thermal Power 591.4 MW
- Core Inlet Temperature 275°C
- Recirculation Flow 3600 kg/s
- Xenon Equilibrium

Two different equilibrium cores were chosen. One of the cores was an equilibrium core with SVEA-96 Optima 2 ("Core A") and the other was an equilibrium core with another fuel type with less number of partial length rods ("Core B") and therefore with a smaller Boron reactivity impact caused by the fewer partial length fuel rods.

5.3   CALCULATIONAL MATRIX

5.3.1   POLCA7

The Boron calculations were made at three different state points:

- BOC
- MOC
- EOFP

The BOC core corresponds to 1000 EFPH, MOC core to 8000 EFPH and the EOFP core to 16000 EFPH.

The calculations were performed for Boron concentrations between 0 - 1200 ppm for "Core A" and between 0 – 900 ppm for "Core B."

5.3.2   BISON

The Boron calculations in BISON were performed at the same state points and Boron concentrations as in POLCA7. The only additional input to BISON is the initial Boron concentration Bppm0, as described in Section 4.1.2 of this report. Only steady state calculations are performed for this validation.

5.4   CALCULATIONAL RESULTS

5.4.1   POLCA7

The results from the POLCA7 calculations are presented in Tables 5-1 to 5-6. The impact on k_{eff} from Boron, Δk_{eff}, is calculated according to:

$$\Delta k_{eff} = (k_{eff(0\,ppm)} - k_{eff}) / k_{eff(0\,ppm)} \tag{5.1}$$

where

$k_{eff(0\,ppm)}$	k_{eff} with 0 ppm Boron concentration
k_{eff}	k_{eff} with a Boron concentration of X ppm
Δk_{eff}	the differential impact on k_{eff} from Boron

The resulting Δk_{eff} are presented in the tables below for both core types ("Core A" and "Core B") at each state point studied (BOC, MOC and EOFP):

Table 5-1	POLCA7 Results for Core A at BOC	a,c

Table 5-2	POLCA7 Results for Core A at MOC	a,c

Table 5-3   POLCA7 Results for Core A at EOFP

a,c

Table 5-4   POLCA7 Results for Core B at BOC

a,c

Table 5-5	POLCA7 Results for Core B at MOC	a,c

Table 5-6	POLCA7 Results for Core B at EOFP	a,c

5.4.2 Results BISON

The cores are collapsed into BISON. The Boron cross-sections used, are valid for a fuel type with 100 full length rods in each assembly (SVEA-100 core). This will lead to a k_{eff} that differ between BISON and POLCA7 when Boron is simulated through different ppm levels.

The results from the BISON calculations are presented in Tables 5-7 to 5-12. The impact on k_{eff} from Boron, Δk_{eff}, is calculated according Equation 5.1.

The resulting Δk_{eff} values are presented in the tables below for both core types ("Core A" and "Core B") at each state point studied (BOC, MOC and EOFP) respectively:

Table 5-7   BISON Results for Core A at BOC

a,c

Table 5-8   BISON Results for Core A at MOC

a,c

Table 5-9   BISON Results for Core A at EOFP

a,c

Table 5-10   BISON Results for Core B at BOC

a,c

Table 5-11	BISON Results for Core B at MOC	a,c

Table 5-12	BISON Results for Core B at EOFP	a,c

5.5 COMPARISONS BETWEEN POLCA7 AND BISON

The obtained Δk_{eff} values presented for POLCA7 in Section 5.4.1 and for BISON in Section 5.4.2 are now compared as ratios representing the reactivity impact from Boron on the two codes. This ratio, defined as EB3d in Equation 4.3, is calculated as:

$$[$$

$$]^{a,c}$$

Results are presented in Table 5-13 for "Core A" and Table 5-14 for "Core B."

Table 5-13   EB3d Ratio between Δk_{eff} for POLCA7 and BISON for Core "A" (a,c)

Table 5-14	EB3d Ratio between Δk_{eff} for POLCA7 and BISON for Core "B"			a,c

5.6 DISCUSSION

The BISON core is based a collapsed POLCA7 core, but with Boron differential cross-sections for a SVEA-100 equilibrium core as opposed to SVEA-96 Optima2, that in addition to the difference in core modeling accuracy introduced by the parallel channel modeling in POLCA7 will lead to a difference in the results between BISON and POLCA7.

[

]^{a,c}

5.7 CONCLUSIONS

From the discussion in the previous section, the following overall conclusions can be drawn:

- The BISON Boron model is verified by comparing the impact on the reactivity with POLCA7.

- A 3D correction term in the Boron model can be maintained constant during an ATWS transient since the BISON results show only an insignificant difference in the Boron reactivity impact when compared with POLCA7.

- The use of a generic set of cross-sections adjusted to a specific core and cycle exposure by the EB3d factor in BISON, is shown to be accurate when compared to the results obtained with the 3D core simulator POLCA7. Expected uncertainty is within a [   ]^{a,c} compared to POLCA7 calculations of Δk_{eff}.

- The BISON Boron model is shown to be verified and validated.

6 ATWS APPLICATION

6.1 BACKGROUND

The Westinghouse strategy for handling the ATWS analysis for a reload is based on comparative studies of the plant response through the [   ]^{a,c} of the licensing basis event for a core [   ]^{a,c}. The limiting transient according to the specific plant's licensing basis is used as the reference case for ATWS.

To illustrate the ATWS application when the analysis of the Boron injection phase is included, the event "Pressure Regulator Failure – open to maximum demand" (PRFO) combined with the failure of the scram system is considered. The analysis is performed for a SVEA-96 Optima2 equilibrium core.

[

]^{a,c}

The methodology for the containment analysis is described in a separate topical report.

6.2 ACCEPTANCE CRITERIA

An ATWS event is defined as any anticipated transient event followed by the failure of the automatic reactor shutdown. ATWS events are considered beyond design basis accidents. The acceptance criteria of the design basis accidents are normally applied to the ATWS evaluation. However, ATWS events are not regarded as design basis accidents from other aspects, such as the application of the single failure criterion.

The ATWS acceptance criteria are according to Reference 3 (page 93) the following:

1. Peak reactor vessel bottom pressure less than 120% of vessel design pressure
2. Peak cladding temperature below 2200°F
3. Peak containment pressure shall not exceed Containment Design Limit
4. Dose below Guideline values of 10 CFR 100
5. Demonstrated equipment availability

6.3 CALCULATIONS

The ATWS calculations are divided into three phases. In the first phase [

]^{a,c}

[

]^{a,c} Figure 6-1 shows the three different phases of the calculations.

a,c

Figure 6-1 The Three Phases of the ATWS Calculation

6.3.1   Phase One

[

]^{a,c}

[

]^{a,c} Figure 6-2 shows the Peak RPV bottom pressure obtained with the cross sections calculated with methods B and C. Figure 6-3 shows the integrated flow through the relief and safety valves and Figure 6-4 shows the average core power.

a,c

Figure 6-2 Peak RPV Bottom Pressure, Cross Sections Calculated with Methods B and C

a,c

Figure 6-3   Integrated Flow Thorough Relief and Safety Valves, Cross Sections Calculated with Methods B and C

a,c

Figure 6-4 Average Core Power, Cross Sections Calculated with Methods B and C

[

$]^{a,c}$

6.3.2 Phase Two

[

$]^{a,c}$

An example of the peak pressure calculation for a hypothetical plant A and "Core A" is given in
Figure 6-5. The peak pressure at the bottom of the reactor vessel is shown for three different burnups:
Beginning of Cycle (BOC), Middle of Cycle (MOC) and End of Full Power (EOFP). The acceptance
criterion (1500 psig for this particular case) is also shown.

a,c

Figure 6-5 Example of Peak Pressure Calculation

Other key parameters are shown in Figure 6-6.

a,c

[

Figure 6-6 Steam Flow, Average Core Power, Void and Core Flow

[

]^{a,c}

a,c

Figure 6-7 CPR Curve and Time when Dryout Occurs

[

]^{a,c} An example of the peak cladding temperature is shown in Figure 6-8.

a,c

Figure 6-8 Peak Cladding Temperature

6.3.3 Phase Three

[

]^{a,c}

Figure 6-9 Different Steps of the ATWS Transient Calculations

[

]^{a,c} The core flow is shown in Figure 6-12 and the relative core power is shown in Figure 6-13.

a,c

Figure 6-10 Steam Flow from Reactor and Flow through Relief and Safety Valves

a,c

Figure 6-11 Steam Dome and RPV Bottom Pressure

a,c

Figure 6-12 Core Flow

a,c

Figure 6-13 Relative Core Power

[

$]^{a,c}$

BISON calculates the flow through the relief and safety valves and the energy released to the suppression pool during the whole transient as shown in Figure 6-16 and in Figure 6-17.

a,c

Figure 6-14 Amount of Boron Solution Injected

a,c

Figure 6-15 Downcomer Two-Phase Water Level

a,c

Figure 6-16 Integrated Flow through Relief and Safety Valves

a,c

Figure 6-17 Amount of Energy Released to the Suppression Pool

The Benchmarking of BISON versus POLCA7 for the Boron calculations is described in Section 5 of this report.

[

]^{a,c} The suppression pool temperature for the example considered here is shown in Figure 6-18.

a,c

Figure 6-18 Suppression Pool Temperature

6.4   CONSERVATIVENESS OF THE PERFECT MIXING MODEL

Figure 6-19 shows the conditions in the reactor during an ATWS after the feed water pumps are tripped and the water level in the downcomer has been reduced to slightly above the top of the active fuel.

[

]ᵃ,ᶜ

a,c

Figure 6-19 Thermal Hydraulic Conditions in the Reactor Pressure Vessel during ATWS

7 SUMMARY

The main purpose of this second supplement to the BISON topical report, Reference 1, is to extend the applicability of the code to the analysis of ATWS sequences beyond the peak pressure calculations performed today to determine the mass and energy release to the containment during the Boron injection phase of the accidents.

This report is structured to complement and augment the original LTR and its supplement described above with the following specific features:

- To extend the maximum approved upper pressure and steam quality limit for the AA78 slip/void correlation.

- To model the reactivity impact from Boron injection during an ATWS transient.

- To describe the application of BISON to ATWS calculations during the Boron insertion phase.

The boron reactivity model implemented uses a conservative modeling of the concentration of Boron in the core and generates conservative mass and energy released to containment. The conservatism achieved is based on two major contributions

[

$]^{a,c}$

8 REFERENCES

1. Topical Report RPA 90-90-P-A, Rev. 0, "BISON – A One Dimensional Dynamic Analysis Code for Boiling Water Reactors"

2. Topical Report CENPD-292-P-A, "BISON – A One Dimensional Dynamic Analysis Code for Boiling Water Reactors: Supplement 1 to Code Description and Qualification," July 1996

3. Topical Report CENPD-300-P-A, Rev. 0, "Reference Safety Report for Boiling Water Reactor Reload Fuel," July 1996

4. Topical Report RPB 90-93-P-A, "Boiling Water Reactor Emergency Core Cooling System Evaluation Model: Code Description and Qualification"

5. Topical Report RPB 90-93-P-A, Rev. 0, "Boiling Water Reactor Emergency Core Cooling System Evaluation Model: Code Description and Qualification"

6. G. S. Lellouche, B. A. Zolotar, "A Mechanistic Model for Predicting Two-Phase Void Fraction for Water in Vertical Tubes, Channels, and Rod Bundles, Electric Power Research Institute," EPRI NP-2246-SR, 1982

7. Martin, R., "Mesure de Tauxde Vide a Haute Pression dans un Canal Chauffant," University of Grenoble, 1967

8. Paul Coddington and Rafael Macian, "A Study of the Performance of Void Fraction Correlations used in the Context of Drift-Flux Two-Phase Flow Models," Nuclear Science Engineering and Design, 215 (2002) 199-216

9. Letter from P. R. Simpson (Exelon Nuclear) to U.S. NRC, "Request for License Amendment Regarding Transition to Westinghouse Fuel," June 15, 2005

10. Topical Report CENPD-390-P-A, "The Advanced PHOENIX and POLCA Codes for Nuclear Design of Boiling Water Reactors," December 2000

11. Topical Report WCAP-16608-P, "Westinghouse Containment Analysis Methodology," August 2006

12. Quad Cities 1 & 2 FSAR, B 3.1.7 Standby Liquid Control (SLC) System